Design and Simulation of a

MEMS-based Piezoelectric Power Generator

by

Tania Tracy anak Baring

Dissertation submitted in partial fulfillment of

the requirements for Bachelor of Engineering (Hons)

(Electrical and Electronics Engineering)

MAY 2011

Universiti Teknologi PETRONAS

Bandar Seri Iskandar

31750 Tronoh

Perak Darul Ridzuan

CERTIFICATION OF APPROVAL

Design and Simulation of a MEMS-based Piezoelectric Power Generator

by

Tania Tracy anak Baring

A project dissertation submitted to the

Electrical and Electronics Engineering Programme

Universiti Teknologi PETRONAS

in partial fulfilment of the requirement for the

BACHELOR OF ENGINEERING (Hons)

(ELECTRICAL AND ELECTRONICS ENGINEERING)

Approved by,

_____

(ASSOC. PROF. DR. JOHN OJUR DENNIS)

UNIVERSITI TEKNOLOGI PETRONAS

TRONOH, PERAK

May 2011

CERTIFICATION OF ORIGINALITY

This is to certify that I am responsible for the work submitted in this project, that the original work is my own except as specified in the references and acknowledgements, and that the original work contained herein have not been undertaken or done by unspecified sources or persons.

_____

TANIA TRACY ANAK BARING

ABSTRACT

Wireless node sensor network are fast becoming a popular option in commercial technology advancements, particularly in the equipment or process monitoring. To power these appliances, batteries are usually used to run the devices. Currently, researchers are looking into the possibility of converting the environment vibration energy (from vibration sources e.g. industrial machines, transportation vehicles) into a low power electric energy, sufficient enough to activate and run the sensors. In this project, the mechanism for piezoelectricity power generation was studied, with the view of integrating into a MEMS-based power generating chip. The design and mathematical formulation are put together before simulating the device using the *CoventorWare* software. At the end of the project, an optimized design should be achieved, in addition to device simulations to verify its performance. This will enable engineers in creating the ideal MEMS-based piezoelectric device in the future.

TABLE OF CONTENTS

LIST OF FIGURES

LIST OF TABLES

ABBREVIATIONS AND NOMENCLATURES

MEMS	Micro-Electro-Mechanical Systems
PZT	Lead-zirconate-titanate
AC	Alternate current
DC	Direct current
A(x)	Beam cross section area
h_y	Beam width
h_z	Beam thickness
l	Beam length
M(x,t)	Bending moment
E	Young's modulus
I	Moment of inertia
$\in$	Magnitude strain of beam
ρ	Density
A	Cross section area
m	Mass
k	Stiffness
ω	Frequency
U(t)	Potential energy
T(t)	Kinetic energy
W(t)	Work done
MPD	Material Properties Database
FEM	Finite Element Method
DTMOS	Dynamic Threshold-voltage MOSFET
MOSFET	Metal-oxide-semiconductor Field-effect Transistor
SiO_2	Silicon dioxide
PZT	Lead Zirconate Titanate (piezoelectric material)
BPSG	Boro-Phospho-Silicate Glass

ACKNOWLEDMENT

CHAPTER 1

INTRODUCTION

1.1 Background Study

1.1.1 Piezoelectricity

Piezo in Greek means pressure, which derives the term *piezoelectricity* meaning "electricity by pressure" [1]. The Piezoelectric effect is a method of converting vibration energy from mechanical strains to electrical potential energy, by means of exploiting piezoelectric materials such as single-crystal quartz, single-crystal Rochelle salt, barium titanate ceramics and lead-zirconate-titanate (PZT) ceramics [2].

It is a reversible process whereby in direct process, applied mechanical stress will induce electrical potential energy but in the reverse process, applied electrical power will generate physical stress or strain to the material. It is a popular method in taking good advantage of the available ambient vibration source and converting it to usable electric energy by means of energy harvesting.

1.1.2 MEMS

Micro-Electro-Mechanical Systems (MEMS) is a type of device that incorporates a combination of mechanical elements, sensors, actuators or electronics on a common silicon substrate, prepared through a series of process in wafer fabrication [3]. It allows the fabrication of small structures within micrometer range. There are two available technologies for MEMS chip manufacturing and it is namely

Bulk Micromachining, which utilizes silicon as the mechanical material and Surface Micromachining, where the deposited or grown layers on the silicon are consumed.

1.1.3 Energy Harvesting via MEMS-based Piezoelectric Method

Harvesting ambient vibration energy using piezoelectric MEMS chip is not a new concept to engineers but it has yet to take off as its functions and operations are still being deliberated among experts. Its mechanism is quite simple, where by the vibration energy in environment will cause a good amount of stress/strain in the material in the MEMS device which will generate an expected low power electrical energy for small electronics and wireless sensors applications. There are many piezoelectric structures being studied, such as the cantilever, diaphragm and double support beam, chosen as such to produce the most optimum vibration energy to match the environment vibration source.

1.2 Problem Statement

Powering any type of wireless sensors could be a hassle with the limited power sources available especially when it is out of reach for maintenance. The use of batteries does not offer the ideal solution as it has limited supply of electrical power and will diminish over time. In addition, the use of batteries may bring up environmental concerns on waste disposal waste in the future.

A piezoelectric power generator may be the answer to an infinite energy supply that would be able to power wireless network sensors. The power generator will be integrated in the MEMS fabrication technology, which would welcome the possibility of constructing a micro-generator, small enough to be built into a mobile device. Simulations of the MEMS device can be generated to ensure that the output fulfills the desired generated voltage. In the end, the device can be optimized to achieve better results based on the simulation outcome.

1.3 Objectives

The objectives for the project are as follows:

- To design a MEMS-based piezoelectric power generator and construct a mathematical modeling of the device.
- To simulate of the device characteristics and output behavior.
- To design an output circuit to tap the potential energy harvested by the power generator.

1.4 Project Scope & Deliverables

For this project, the cantilever beam structure will be considered due to its simplicity and compatibility with the MEMS fabrication technology [4]. An array of cantilever will be designed to widen the effective frequency bandwidth for energy harvesting [5] to 200-220Hz based on the mechanical frequency of a computer [6]. Other vibration sources can also be referred to but the computer mechanical frequency is selected as an easy reference. A mathematical analysis will be derived from the design to determine the theoretical output voltage and power, as well as coming up with the most suitable beam dimension to produce close resonant frequencies between the cantilevers. Further study will be conducted on how to overcome the phase difference [5] of the output voltages.

As for device simulations, the project will be focusing more on producing wider effective frequency bandwidth that can be utilized for energy harvesting. Output simulations such as voltage, power and resonant frequency can be generated to show the device capabilities, prior to design optimization.

Besides that, a suitable output circuit will be implemented to the device to obtain a usable voltage output for consumption. The types of circuits that will be looked into are rectifying circuits, voltage multiplying circuit or capacitive smoothening circuit.

CHAPTER 2

LITERATURE REVIEW

2.1   Previous Work on MEMS Piezoelectric Power Generator

There are many available research papers based on piezoelectricity power generation via MEMS fabrication. In one paper, a cantilever structure with a nickel proof mass was designed as a vibration generator structure [7] showed in Figure 2.1.
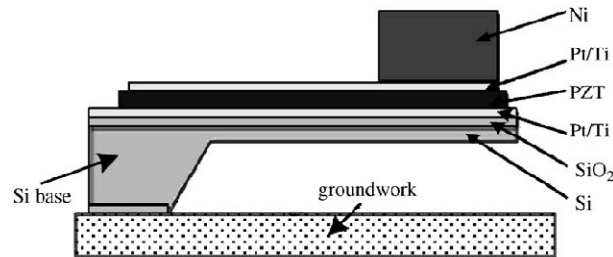
Figure 2.1: Cross sectional sketch of the prototype [6]

The prototype was able to generate 898mV voltage and 2.16µW power output, which manages to overcome the germanium diode rectifier system where it would convert the generated AC supply to DC. However it is still deemed insufficient for general use as the effective energy harvesting bandwidth is too narrow, which is less than tens Hz close to the resonant point.

Hence, another research paper on an array of cantilever piezoelectric MEMS generator is brought up [5]. This is to address on the common result of piezoelectric devices having a narrow effective energy harvesting bandwidth as this causes inefficiency in energy harvesting and energy conversions. Consequently, a set of cantilevers were fabricated with close resonant frequencies, arranged in a series as shown in Figure 2.2.
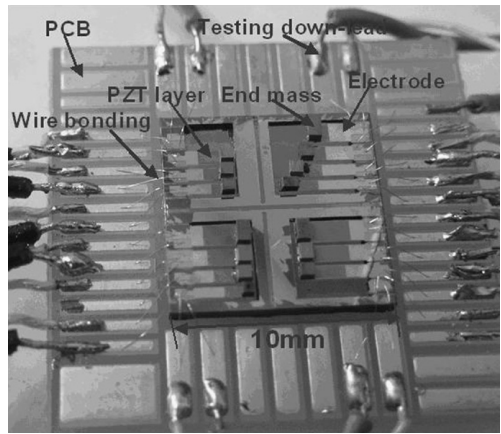
Figure 2.2: Array of cantilever prototype design [5]

This would allow some flexibility in the effective harvesting frequency bandwidth. The prototype device produced resonant frequencies between 226 – 234 Hz, producing an improved combination power output of 3.98μW and 3.93 DC output voltages. However, the combined output power value is not precisely the summed up theoretical values of the cantilever structure device as there were a phase difference of nearly 120º of the generated voltage output.

Another paper presented an approach on having four cantilever type devices with two cantilevers for d31 and d33 configuration mode respectively [8]. Configration mode for d31 consists of a piezoelectric layer, sandwiched between two metal electrodes while d33 has a interdigitated electrode on top of the piezoelectric layer. The configuration mode diagram can be referred to in Figure 2.3.
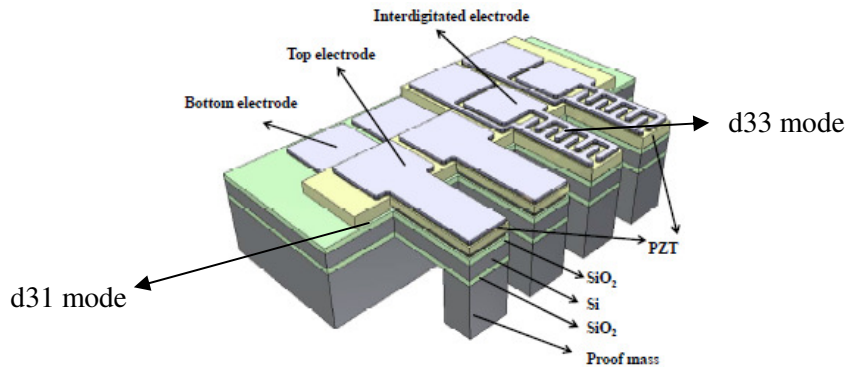
Figure 2.3: Configuration mode of d31 and d33 [8]

The combination of operation modes also presents as another solution in widening the effective bandwidth for vibration energy harvesting. The prototype successfully produced a wider range of frequency that is between 237 – 244.5 Hz. The output voltages and power were presented in another paper.

The selection of the most suitable operation mode is also taken into account. A MEMS power generating device using PZT thin film [9] was designed which employed the d33 operation mode. The particular operation mode was chosen because d33 mode could generate up to 20 times higher voltage than d31 mode, based on a study regarding high sensitivity sensors with piezoelectric elements in [10, 11]. It is found that the length of cantilever beam can be extended to be much longer for the case of d33 but d31 mode is limited to the thickness of the PZT layer. Figure 2.4 shows the configuration differences between the 2 modes.
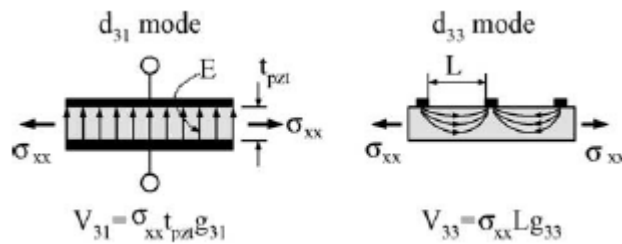
Figure 2.4: d31 mode can be varied by thickness while d33 mode can be varied by length [9].

Next, an authentic piezoelectric cantilever bimorph micro transducer electro-mechanical energy conversion model was designed, taking up the curvature basis approach in its analytical modeling [12]. Two transducers cluster were designed at the same length but different width as well as different length but same width. In this model, the relationship between induced vibration voltage, mechanical strain and piezoelectric polarization is established using the curvature basis approach. The damping effect was also considered during the testing of the device. Results shows that the maximum induced voltage is unrelated to the cantilevers width, proportional

to the excitation frequency but is inversely proportional to the length of the structure and the damping factor.

Finally, a comparative study was also conducted on the previous works on the design and fabrication techniques for the piezoelectric harvesters [4]. It is found that the d31 operation mode has greater advantage towards energy harvester by MEMS-based technology as its resonant frequency is lower compared to the d33 mode, matching the low frequencies from the ambient environment. Output power does not depend on the type of operation mode but it is mainly due to project conditions such as resonant frequency, acceleration, input vibration and proof mass. Using PZT as the piezoelectric material, attaching the most optimum weight for a proof mass, low resonant frequency and bigger gaps between the interdigitated electrodes can help in improving the design of a piezoelectric power generator.

2.2   The Piezoelectric Effect

A simplified look on how the piezoelectric mechanism works on a crystal structure can be found in Figure 2.5 and 2.6 [13]:

a) The charges in a piezoelectric crystal are exactly balanced, though they are not arranged symmetrically. Hence, the electric dipole moment of the charges cancels out each other, producing no net charge on the crystal surfaces.
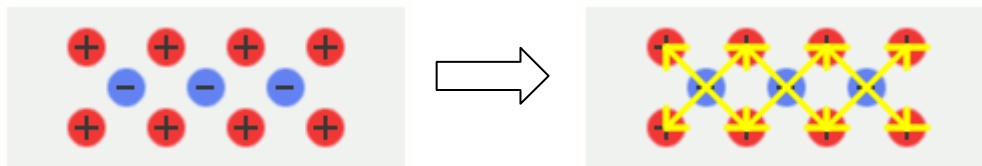
Figure 2.5: Atoms in its normal structure state where its electric dipole moment cancels one another. [13]

b) When force is exerted on the crystal, the charges are displaced and out of balance. In this case, the electric dipole moments no longer cancel each other out and forms positive and negative charges on each of the crystal surface.
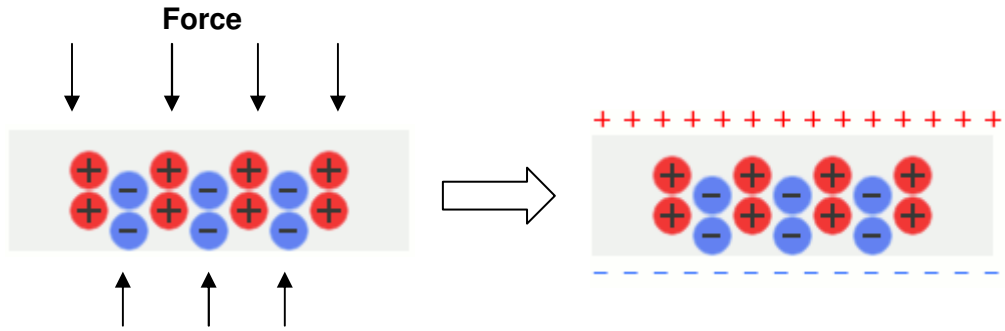
Figure 2.6: Force is exerted onto the structure and produces opposing charges on the crystal surface [13].

2.3   Theory in Mathematical Modeling

2.3.1   Euler Bernoulli Beam Equation

To further understand the dynamic behavior of the cantilever beam device, the elementary *Euler-Bernoulli* beam equation is studied. The assumptions used in formulating the mathematical model are that the beam be [14]:

- Uniformed along its span, or length and slender.
- Composed of a linear, homogenous, isotropic elastic material without axial loads.
- The plane sections remain plane.
- The plane of symmetry of the beam is also the plane of vibration so that rotation and translation are decoupled.
- The rotary inertia and shear deformation can be neglected.

A model of a vibrating beam structure is as shown, in Figure 2.7:
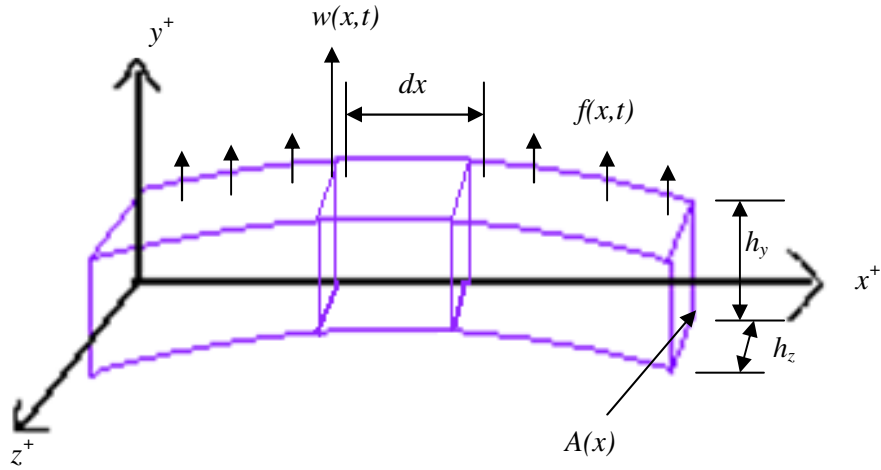
Figure 2.7: Simple Euler-Bernoulli beam of length *(l)* in vibrating in transverse direction [14]

The beam has a rectangular cross section *A(x)* with width h_y, thickness h_z and length *(l)*. Also associated with the beam is the bending stiffness *EI(x)*, where E is the Young's elastic modulus for the beam and *I(x)* is the cross-section area moment of inertia about the *z*-axis.

Bending moment *M(x, t)* is affected by beam deflection *w(x, t)* by

$$M(x,t) = EI(x)\frac{\delta^2 w(x,t)}{\delta x^2} \tag{1}$$

While the magnitude strain of the beam [14] is affected by

$$\in = -z\frac{\delta^2 w(x,t)}{\delta x^2} \tag{2}$$

A model of a vibrating beam structure may be developed from studying the force diagram of an infinitesimal element of the beam [14], as shown in Figure 2.8.

The flexing of the beam is assumed to be small enough such that the shear deformation is much smaller than *w(x, t),* so that the sides of the element do not bend.
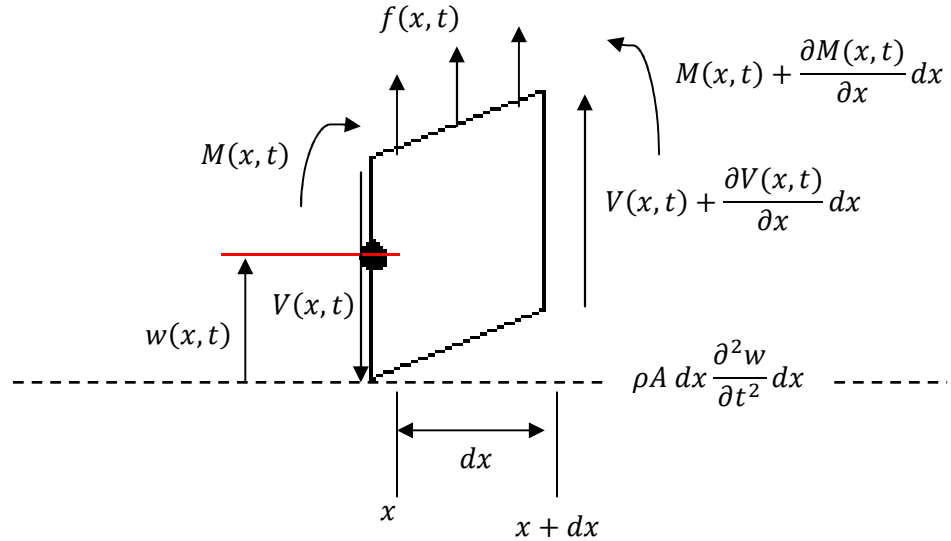
Figure 2.8: Free-body diagram of a small element of the beam as it is deformed by a distributed force per unit length, *f(x,t)* [14]

If no external force is applied so that *f(x,t)* = 0 and that *EI(x)* and *A(x)* are assumed to be constant, the free vibration equation is simplified as

$$\frac{\delta^2 w(x,t)}{\delta t^2} + c^2 \frac{\delta^4 w(x,t)}{\delta x^4} = 0 \tag{3}$$

Where $c = \sqrt{\dfrac{EI}{\rho A}}$ (4)

Equation contains 4 spatial derivatives and hence requires four boundary conditions to calculate its solution. The boundary conditions required to solve the spatial equation of the beam are:

a) the deflection *w(x,t)*

b) the slope of the deflection $\dfrac{\delta w(x,t)}{\delta x}$ (5)

c) the bending moment, $\dfrac{EI\delta^2 w(x,t)}{\delta x^2}$ (6)

d) the shear force, $\dfrac{\delta \dfrac{EI\delta^2 w(x,t)}{dx^2}}{dx}$ (7)

The conditions are determined by the beam configuration design, whether it is clamped-end (fixed end), pinned end or free end. For the case of a cantilever beam where the beam is free at one end, the deflection and slope at the end is unrestricted but the bending moment and shear force is made to be equal to zero:

Bending moment = $EI \dfrac{\partial^2 w}{\delta x^2} = 0$ (8)

Shear of force = $\dfrac{\partial}{\delta x}\left[EI \dfrac{\partial^2 w}{\delta x^2} \right] = 0$ (9)

As work is done by external forces of the design, the system's potential energy, kinetic energy and work done is derived as follows [14]:

Potential energy: $U(t) = \dfrac{1}{2}\int_0^L EI\left(\dfrac{\partial^2 w}{\delta x^2}\right)^2 dx$ (10)

Kinetic energy: $T(t) = \dfrac{1}{2}\int_0^L \rho A\left(\dfrac{\partial w}{\delta x}\right)^2 dx$ (11)

Work: $W_f(t) = \int_0^L f_c(x,t).w(x,t)dx$ (12)

11

Where if gravity is the only distributed conservative load acting on the beam,

$$f_c(x,t) = \rho(x)A(x)g \tag{13}$$

2.3.2 Beam free vibration frequency

Using distributed parameter modeling, the free vibrations of a long simple cantilever may be obtained [15]. Similar to Equation (3), when the cross section of the beam in constant, it would result to the equation (14):

$$EI\frac{\delta^4 w(x,t)}{\delta x^4} + \rho A\frac{\delta^2 w(x,t)}{\delta t^4} = 0 \tag{14}$$

Using the separation of variables method, it is assumed that

$$w(x,t) = W(x)T(t) \tag{15}$$

By means of *w(x)* for *W(x)*, the following equation can be derived from Equation (14) and (15):

$$\frac{\delta^4 w(x,t)}{\delta x^4} - \beta^4 w(x) = 0 \tag{16}$$

where

$$\beta^4 = \frac{\rho A \omega^2}{EI} \tag{17}$$

The general solution that can be obtained as shown in *Balachandran* [15], which are in the form of:

$$w(x) = A\cosh(\beta x) + B\sinh(\beta x) + C\cos(\beta x) + D\sin(\beta x) \tag{18}$$

For a cantilever of length l with fixed-free ends, the following equation is obtained by applying the boundary conditions in Equation (8) and (9):

$$1 + \cosh(\beta l)\cos(\beta l) = 0 \tag{19}$$

Hence, the following solutions are obtained which describes the first three modes [14]:

$$\beta l = \begin{cases} 1.8751 \\ 4.6941 \\ 7.8547 \end{cases} \tag{20}$$

Combining the definition of β in Equation (17) and the values of βl using the first mode in Equation (20), the natural frequency corresponding to the first mode is

$$\omega = 3.52\sqrt{\frac{EI}{ml^3}} \tag{21}$$

Where m is the effective mass of the cantilever system,

$$m = \frac{\rho}{A} \tag{22}$$

2.3.3   Bending frequency of a beam cantilever

Figure 2.9 shows a simple cantilever beam structure. The dimensions w, t, and l represents the width, thickness and length of the beam respectively.
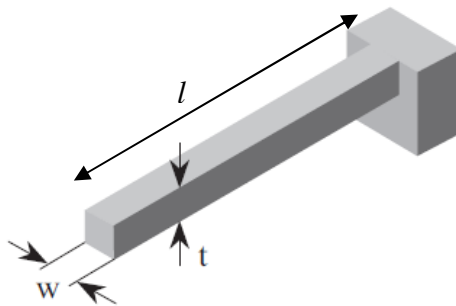
Figure 2.9: Simple beam structure [16]

Based on the Euler-Bernoulli beam model, the moment of inertia for the beam is [1]

$$I = \frac{wt^3}{12}$$

(23)

The spring constant constant is adapted from Hooke's law which is

$$F = kx$$

(24)

and it presents the spring constant of the beam as [1]

$$k = \frac{F}{x} = \frac{3EI}{l^3} = \frac{E(wt^3)}{4l^3}$$

(25)

where E is the Young's Modulus of the beam.

The effective mass of the cantilever beam can easily be found as

$$m = \rho \times l \times w \times t$$

(26)

where ρ is the density of the elastic substrate of the beam. The calculation for the added mass uses the same formula as well.

The natural frequency of the bending cantilever can be found as [1]

$$f = \frac{\omega}{2\pi}$$

(27)

where

$$\omega = \sqrt{\frac{k}{m}}$$

(28)

Adding the added mass into the equation (28) for cantilever beams with tip mass, the shifted frequency for the cantilever becomes [1]

$$f = \frac{\omega}{2\pi} = \frac{\sqrt{\dfrac{k}{m + \Delta m}}}{2\pi}$$

(29)

2.3.4   Bending frequency of a multimorph cantilever

Based on Figure 2.9 by *Lobontiu* [16], the bending frequency of a beam consisting of different layers with the same length can be calculated based on a lumped-parameter model. Figure 2.10 shows the parameters needed for calculation.
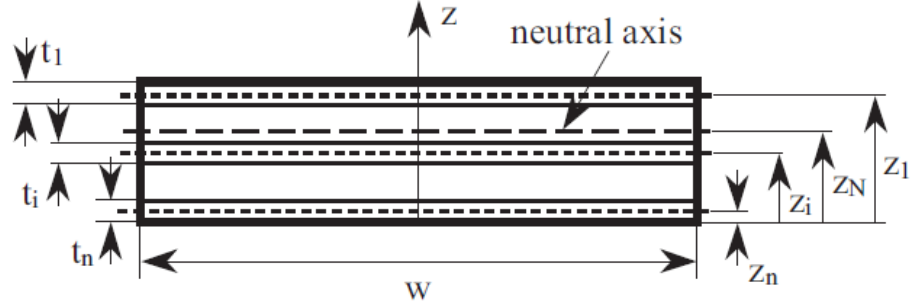
Figure 2.10: Cross section of a multi-morph beam with main geometry parameters for bending frequency calculations [16]

As shown by *Lobontiu* and *Garcia* [17], the equivalent bending rigidity can be obtained as

$$(EI_y)_e = \sum_{i=1}^{n} E_i [I_{yi} + z_i A_i (z_i - z_n)] \tag{30}$$

where I_{yi} is moment of inertia of the *i*th component with respect to its central axis y_i.

The position of the neutral z_n is calculated as [16]

$$z_n = \frac{\sum_{i=1}^{n} z_i E_i A_i}{\sum_{i=1}^{n} E_i A_i} \tag{31}$$

The stiffness of the multi-morph cantilever is [16]

$$k_{b,e} = \frac{3(EI_y)_e}{l^3} \tag{32}$$

The distributed mass of the beam is given as [16]

$$m_{b.e} = \frac{33l \sum_{i=1}^{n}(\rho_i A_i)}{140} \tag{33}$$

Then the bending resonant frequency can be easily calculated using [16]

$$\omega_{b,e} = \sqrt{\frac{k_{b,e}}{m_{b.e}}} = 3.567 \sqrt{\frac{(EI_y)_e}{l^4 \sum_{i=1}^{n}(\rho_i A_i)}} \tag{34}$$

2.3.5 *The output voltage of the cantilever beam with added mass*

Figure 2.11 shows the geometries of a simple cantilever beam with tip mass.
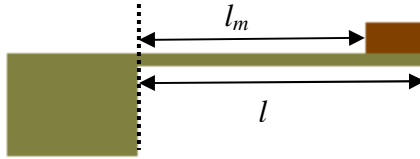
Figure 2.11: Geometry parameters of a cantilever beam with tip mass.

To calculate the output voltage that can be generated by the cantilever at steady state, the bending moment, beam deflection and the maximum stress of the beam must be calculated first.

The bending moment can be found as [18,19]

$$M = \Delta m \times g \times l_m \tag{35}$$

where l_m representing the distance from the fixed end to the mass, g is the acceleration of gravity (9.81ms^{-2}) and Δm is the added mass.

The deflection of the beam can then be calculated as [18]

$$Y = \frac{\Delta m \times g \times L^3}{3EI} \tag{36}$$

Substituting equation (23) into (36) we have

$$Y = \frac{4 \times \Delta m \times g \times L^3}{Ewt^3} \tag{37}$$

Thus the maximum stress is found to be [20]

$$\sigma_{max} = \frac{3Et}{2L^2} Y \tag{38}$$

The output voltage of the cantilever power generator can then be calculated as [21]

$$V_{oc} = g_{31} \times \sigma_{max} \times t_p \tag{39}$$

where g_{31} is the piezoelectric constant of the piezoelectric material and t_p is the thickness of the piezoelectric layer.

2.4   CoventorWare

CoventorWare is an integrated suite of tools designed to produce accurately modeled MEMS and microfluidic design [22]. The software is capable of producing a representation model of a device and run device simulations based on the material properties and structure characteristic being input into the software. The major components that make up the software are as below:

2.4.1   Material Properties Database (MPD)

When creating a design, the first step to be done is to declare the materials properties and characteristics into the database. The database stores materials that will be used for design and the properties are keyed in following the user's design model. Only the materials in the database are accessible in the Process Editor.

2.4.2   Process Editor

The process editor allows users to create a process flow representing the foundry process that will fabricate the device. Materials, mask names, film deposit and etch profiles are entered into the process flow using basic sequence of depositing and etching steps. The material selected in the design is dependent on the Material Properties Database which stores all materials and its associated properties to properly simulate the process.

2.4.3   Architect

The Architect simulates design configuration using the system-level approach. It uses the information in MPD and process files in its simulation. Users can employ high-level design techniques to create a system model that can be simulated using the schematic capture. In Architect, simulation software can be used to simulate the schematic under various user-defined conditions and plotting tools are used to view and measure results in several graphical formats. The schematic model can be build using generic library parts, custom electromechanical, optical, magnetic or fluidic parametric libraries as well as user generated macromodels.

2.4.4   Designer

The Designer tool can be used to extract MEMS design from an Architect schematic or to build a device from a process file and a 2-D layout. To create a 2-D layout, the CoventorWare's Layout Editor can be utilized to do some comprehensive drawing to create the 2-D layout. The completed process description from Designer will be used to build a 3-D model with the assistance of Preprocessor visualization module.

2.4.5   Meshing

Meshing divides and performs model calculations the solid 3-D model. The resulting mesh obtained can be used by the Analyzer solvers for Finite Element Method (FEM) simulations.

2.4.6   Analyzer Modules

The Analyzer Modules sets boundary conditions and selects appropriate solvers to perform FEM. Solver data can be used to vary process parameters, iterating runs or by curve-fitting the prior result to produce the best design optimization. Examples of some of the solvers available that is related to the project are:

  ➢ Deformations from applied pressure or forces.
  ➢ Solutions using full contact boundary conditions.
  ➢ Modal analyses of the natural vibration frequencies of modeled mechanical devices.
  ➢ Calculation of damping effects on MEMS device behavior.

2.4.7   Integrator

This tool extracts reduced-order macromodels to be used in system simulation. From the Analyzer solver menus, it allows the creation of macromodel representing spring stiffness, damping, inertial and fluid flow effects. The compact models extracted will simulate in less time compared to a normal designed model and can be very useful for complex simulations with electronic components in a MEMS device.

2.5   Output circuit

Various output circuits are implemented in the previous work done by other researchers. The type of output circuit implemented depends on the type of output power desired. One example of an output circuit shown in Figure 2.12 is presented by *J.-Q. Liu et al.* [5] where an AC-DC rectification circuit is employed to achieve higher voltage in their cantilever array design. The output voltage of each cantilever is connected in series and operates just like a serial battery connection. However, it consumes a small amount of power to operate thus reducing some of the output power generated from the cantilevers.
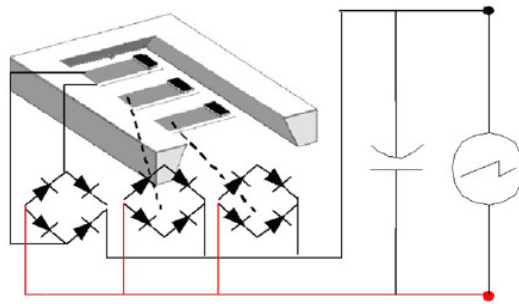
Figure 2.12: AC-DC rectification circuit for cantilever array power generator [5].

Y.B. Jeon et al. [9] incorporated a storage device for their output circuit design of their piezoelectric micro power generator. Their power system is able to produce a DC power output from the AC power generated by their d33 cantilever device using the rectifying circuit and store the generated electric energy in a capacitor as shown in Figure 2.13.
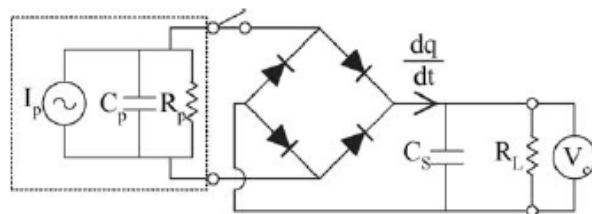
Figure 2.13: Rectifying and storage circuit implemented in generator power system [9].

Another type of output circuit to manage the power generated is the voltage multiplier as discussed by *Hela et al.* [23]. This circuit shown in Figure 2.14 below is generally used to multiply as well as to rectify the output voltage of the micro power generator. In their research, they have proposed and simulated a novel low threshold diode based on DTMOS transistor to overcome the problem of the output voltage of a generator being smaller compared to the threshold voltage of the standard diode.
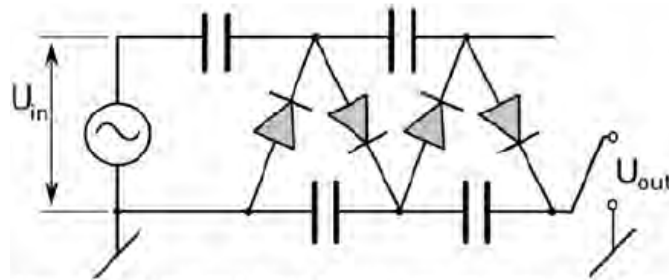
Figure 2.14: Conventional four stage voltage multiplier [23].

CHAPTER 3

METHODOLOGY

3.1 Mathematical modeling for cantilever beam design

In order to come up with a cantilever array with close resonant frequencies characteristics, a proper mathematical calculation was done to obtain the proper beam dimensions. In this project, the *Euler-Bernoulli* beam equation will be the elementary beam theory for the modeling of the device mathematical model.

First, the preliminary dimensions of the cantilever design is established based on previous work findings [4, 5, 7, 8, 12, 14] to produce theoretically the most effective cantilever that can generate low frequency of around 200-220 Hz and a minimum amount of voltage of 2 to 3 volts. Then, the appropriate constants of the cantilever material should be retrieved such as the Young's modulus and density before proceeding to emulate the mathematical model for the cantilever system. The equations can be derived to calculate the natural frequency and deflection of the cantilever design that consists of multiple layers and a proof mass.

For the project design, the modeling takes into account the elastic component of the design which is the thickest among all layers. The elastic component properties will be the main substrate to calculate and estimate beam's stiffness and equivalent mass. The other layers are considered negligible as its thickness is small compared to the main substrate. Next, the mathematical model can be simulated using the dimensions established earlier as well as to obtain several plausible value ranges using the MATLAB software. The software outcome can be considered as the device theoretical result based on an ideal condition.

3.1.1 Preliminary design of the multi-morph cantilever

A multi-morph cantilever consists of several different layers on the beam. For the project design, the beam layers are all equal in length (from the anchor) and width but its material properties will differ. Figure 3.1 shows the multi-morph beam design used in the project while Table 3.1 shows the characteristics of the material.
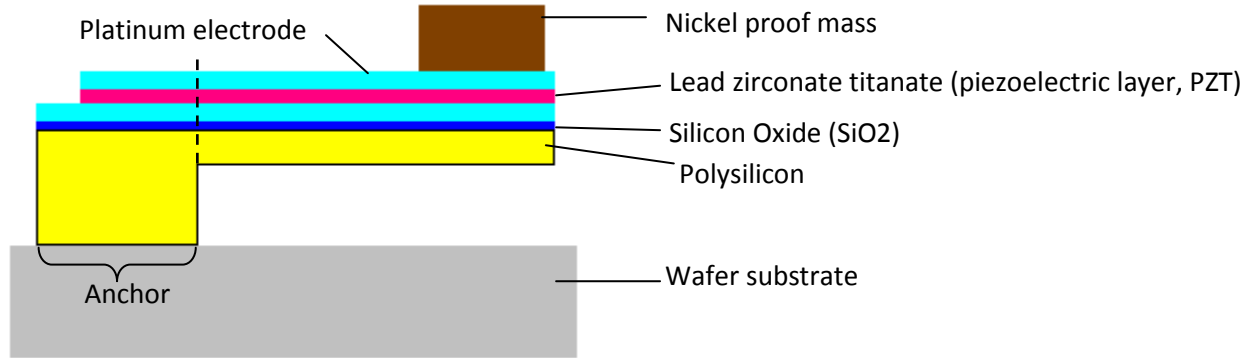
Figure 3.1: Preliminary design of multi layered cantilever with proof mass

Table 3.1: Characteristics of beam material chosen

Material	Characteristics
Polysilicon	• Functions as an elastic component for beam bending.
Silicon Oxide (SiO$_2$)	• Acts as an adhesive for Platinum to adhere to Polysilicon layer. • An insulating layer.
Lead zirconate titanate (PZT)	• Piezoelectric layer. • Generates voltage upon exerted force.
Platinum	• Conducts electricity efficiently.
Nickel	• Unreactive metal.

Figure 3.2 shows the beam geometry parameters for bending frequency calculation parameters while Table 3.2 presents the material properties that can be referred to for calculations in later chapters. Also shown below is Figure 3.3 where the Nickel mass geometry parameter that is used in the device is defined.

0.3μm (Platinum)
2μm (PZT)
0.3μm (Platinum)
2μm (SiO₂)
12μm (Polysilicon)

Width = 500μm
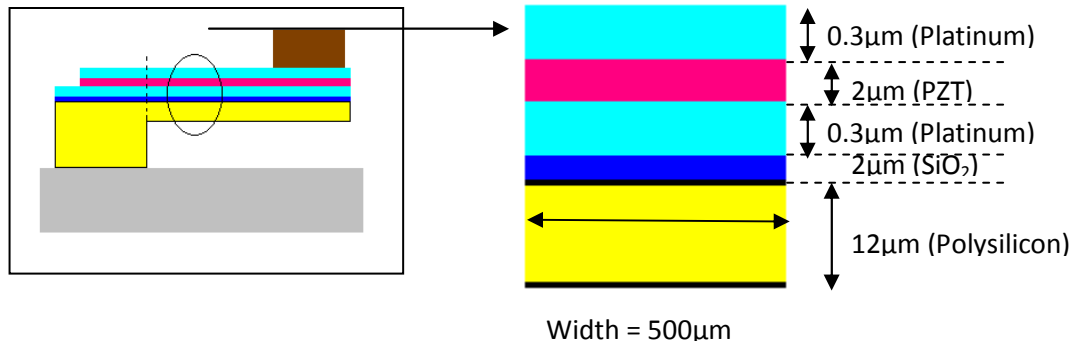
Figure 3.2: Cross section of beam dimension with geometry parameters

Table 3.2: Multi-morph beam material properties for calculation [23]

Property	Polysilicon	SiO$_2$	Platinum	PZT	Nickel
Young's Modulus, E $(10^3$MPa)	160	70	170	89	221
Density, ρ (kg/m^3)	2330	2200	2150	7700	8900

L_{Ni} = 500μm
w_{Ni} = 500 μm
t_{Ni} = 200μm

t_{Ni}
w_{Ni}
l_{Ni}
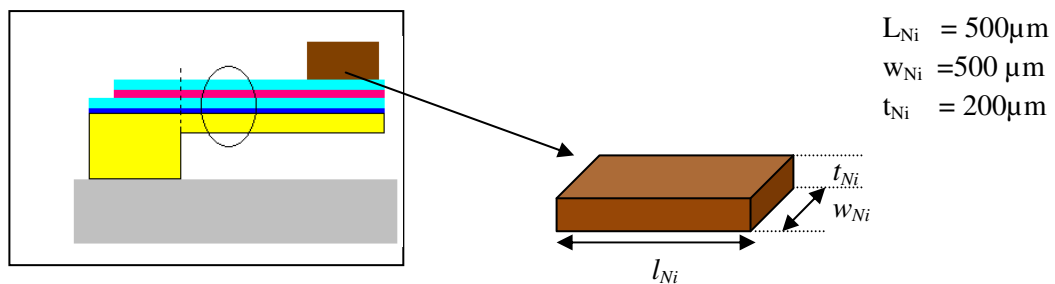
Figure 3.3: Nickel patch geometry parameter

3.1.2 Bending frequency of the power generator cantilever

Consider the elastic component of the beam, consisting of Poly-silicon as shown in Figure 3.4.
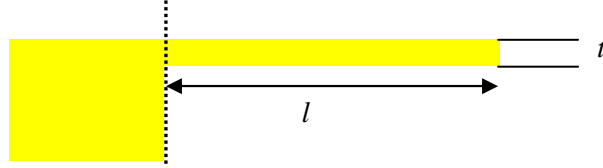
Figure 3.4: Simple cantilever consisting of the elastic component only.

The moment of inertia for the beam is calculated using equation (23) with w as the cross section width of the tip of the beam. The stiffness and effective mass of the beam is then calculated using equation (25) and (26) respectively using the Poly-silicon Young's modulus and density value in Table 3.2.

The added Nickel mass, Δm, at the tip of the beam is calculated using equation (26) as well using the density value of Nickel in Table 3.2 and the geometry parameters showed in Figure 3.3. The mass of the beam and the added mass is summed to obtain the overall effective mass of the cantilever structure where

$$m_{eff} = m + \Delta m$$

(40)

Using the beam stiffness and the sum of the effective mass that has been obtained, the natural frequency of the cantilever beam with added tip mass is calculated using equation (29).

3.1.3 Voltage output calculation of the power generator

The output voltage of the cantilever at steady state can be calculated by obtaining the bending moment, beam deflection and the maximum stress of the beam first.

The bending moment can be calculated using equation (35) where l_m is expressed as

$$l_m = l - l_{Ni} \tag{40}$$

The deflection of the beam is calculated using equation (37) using the Poly-silicon Young's Modulus listed in Table 3.2. Applying the obtained deflection value, the maximum stress can be calculated using equation (38). Finally, the output voltage can then be calculated using equation (39) using the maximum stress value obtained.

3.1.4 MATLAB programming to obtain accurate theoretical values

From the preliminary dimensions, the hand calculated bending frequency obtained from the multi-morph dimensions may not be accurately recorded. Also, a range of dimension needs to be obtained to produce the desired frequency range of 200-220Hz. Thus, MATLAB is used to achieve these values as well as to simulate a suitable dimension range in order to fulfill the requirements needed for the design.

Performing this task required programming the mathematical equations used into the MATLAB script before compiling it to get the wanted result. The script for the simulation can be referred to in the Appendix and the result of the simulation can be viewed in the Chapter 4.
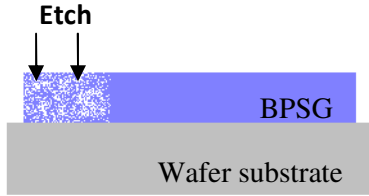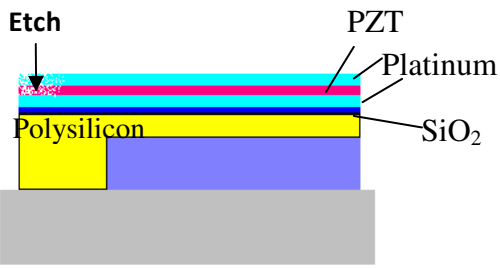
3.2 CoventorWare Design

The simulation result of the device is achieved by designing the layout of the device using the Layout Editor. Next, the process fabrication of the device is defined in the Process Editor to define the layer deposition and etching process. CoventorWare uses the Finite Element Method (FEM) meshing for calculation. Then, the Analyzer Modules are used to apply characteristics solvers for the beam.
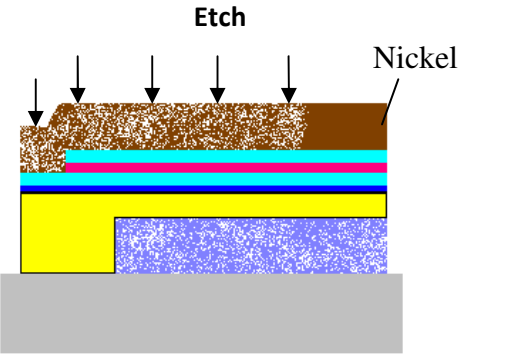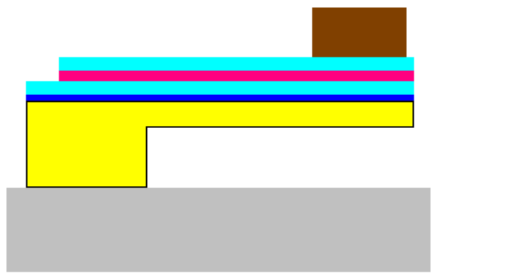
First, properties of the materials used in the design will be keyed into the MPD. The material properties of the cantilever design can be referred to Table 3.2.

Next, the Designer is used to build the design layout with the Layout Editor which will produce a 2-D schematic of the device. The layout of the design represents the mask that is used to build the solid 3D model.

In the Process Editor, a basic fabrication process flow must be created to simulate device manufacturing process. The fabrication process flow for the design is shown in Table 3.3.

Table 3.3: The fabrication process flow for cantilever with added mass design

Process flow	Elabration
	• BPSG is deposited on top of the wafer substrate surface. • A small part of the polysilicon surface is etched for the anchor of the cantilever.
	• Polysilicon is deposited next, filling in the space for the cantilever anchor. • Followed by layers of SiO_2, Platinum, PZT and another layer of Platinum. • A small portion of the PZT and top Platinum layer is etched to make an opening for the electrical connections on the bottom Platinum electrode.

27

Etch Nickel	• Next, Nickel is deposited on top of the layer surfaces. • The portion that is not needed for the cantilever proof mass is etched away. • Then, the BPSG layer underneath the silicon is removed by wet etch method.
	• Finally, the cantilever design is formed.

After the layout and the fabrication process of the design is finalized, the 3-D model of the device can then be generated using the Preprocessor in Designer. Meshing is done only to the moving parts of the design to save time in FEM calculation.

Finally, design output characteristics such as frequency, displacement and stress can be simulated using the Analyzer MemMech solver.

3.3 Output Circuit

Most piezoelectric power generator model presented in the papers [5, 7, 25] have produced AC power as an output. Hence, there is a need to rectify the power to a usable DC power. Various electronic circuits can be used to obtain the best possible usable voltage as the main purpose for this circuit is to rectify the power from the generator from AC to DC power.

For this project, a model of a single phase full wave rectifier circuit was studied to achieve that aim. A look at Figure 3.5 shows an AC source connected to four diodes with a resistive load.
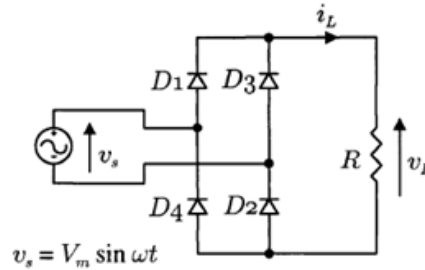
Figure 3.5: Single phase full wave rectifier circuit schematics [26]

In this circuit operation, the current flows to the load through conducting diodes D1 and D2 during the positive half cycle. Diodes D3 and D4 will conduct during the negative half cycle of the AC source. The voltage and current waveforms of the rectifier are shown in Figure 3.6.
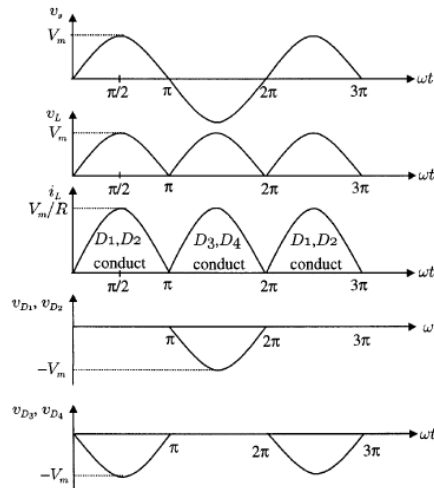
Figure 3.6: Voltage and current waveforms of the circuit [26]

From the voltage output waveform, it can be seen that the AC voltage source can be rectified using this particular circuit where constant positive output voltage

can be achieved. As a modification step, a capacitor can be added into the circuit across the resistive load to achieve a smoother voltage output.

For an array of three cantilevers design, a three phase full wave rectifier will be used to tap the electric power harvested from the devices. This is to address the phase difference made by the different frequencies of the beams as the cantilevers are likely to produce AC power at different phases, as reported by *Liu et al.* [5]. Figure 3.7 presents the three phase full wave rectifier which is to function as a rectifier to produce a usable DC power from beam's AC power output.
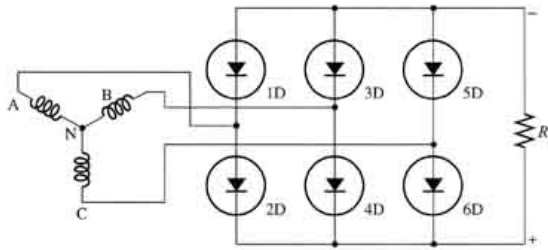
Figure 3.7: Schematic of the three phase full wave rectifier [27]

The circuit in Figure 3.7 shows that the secondary winding of the bridge transformer is connected to the diode rectifier. The anode of 1D, 3D and 5D diodes are connected to the negative DC terminal output power and the cathode of 2D, 4D and 6D diodes to the positive DC output terminal. The operation of the circuit is as follows: the AC voltage output from the power generator device will be connected to the bridge and flowed to any two points of the diode rectifier at one time. At each point, one diode with flow to the negative terminal and the other to the positive terminal respectively, creating a closed circuit. With every phase difference created by the cantilever array, the rectifier circuit will produce an average DC output power from all the phases. This creates a steady DC output power from the rectifier. Figure 3.8 shows an example of the different phases of the phases produced by the cantilever arrays and Figure 3.9 presents the steady output power from the rectifier.
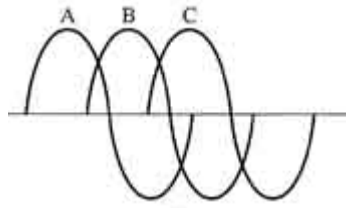
Figure 3.8: An example of the AC output with shifted phases from the cantilever array [27]
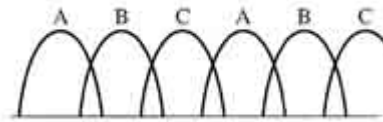
Figure 3.9: The steady DC output power from the rectifier. [27]

CHAPTER 4

RESULTS AND DISCUSSION

4.1   Mathematical Model of Cantilever Beam

4.1.1   Frequency of the cantilever beam with added mass

The calculation for the beam frequency was programmed into MATLAB as a quick and accurate way to obtain the required range of the beam length based on the desired frequencies of 200-220Hz. The equation (23), (25), (26) and (29) was used with the beam length range of 3600 - 4400µm and the other beam geometry parameter in Figure 3.2, 3.3 and Table 3.2. The resulting graph is showed in Figure 4.1. The MATLAB script used to generate simulations for this project can be found in Appendix B.
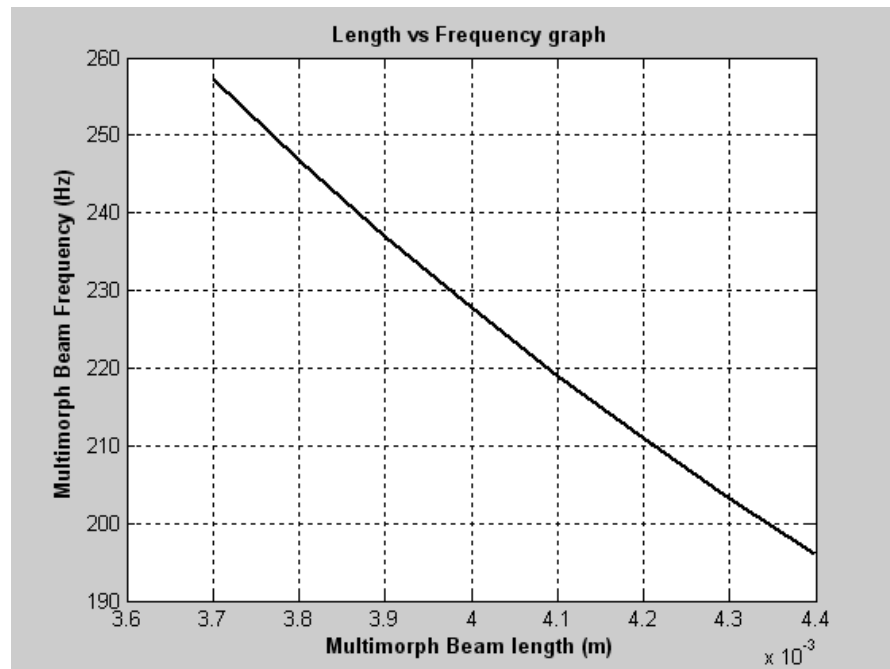
Figure 4.1: Beam length versus frequency graph

From the Figure 4.1, it is observed that the frequency range of 200-220Hz can be obtained using the beam length range of 4150-4350µm. The values for beam stiffness and mass for every beam length and frequency are summarized in Table 4.1.

Table 4.1: Summary of beam calculated parameters

Actual Frequency	Beam length, l (µm)	Beam stiffness, k	Beam mass, m (kg)
200Hz	4340	0.8257	7.5841×10^{-8}
210Hz	4210	0.9046	7.3570×10^{-8}
220Hz	4080	0.9939	7.1298×10^{-8}

The added Nickel mass, Δm, is calculated with equation (26) using its parameters in Figure 3.3, yielding 4.455×10^{-7} kg and it is kept constant throughout the whole calculation. The summation result of the beam mass and the added mass uses equation (40) and it is listed together with the added mass calculated for each frequency in Table 4.2.

Table 4.2: Sum of beam mass and Nickel added mass

Actual Frequency	Δm	$m + \Delta m$
200Hz	4.4550×10^{-7}	5.213×10^{-7}
210Hz	4.4550×10^{-7}	5.191×10^{-7}
220Hz	4.455×10^{-7}	5.168×10^{-7}

4.1.2   *Voltage output of the cantilever power generator*

The output voltage of the cantilever at steady state can be calculated by obtaining the bending moment, beam deflection and the maximum stress of the beam using equation (37), (38) and (39) respectively. Prior to calculating the bending moment, l_m must be calculated first. The summarized values calculated can be found in Table 4.3.

Table 4.3: Summary of beam calculated parameters for beam voltage output

Actual Frequency	l_m (µm)	Bending moment	Beam deflection	Maximum stress
200Hz	0.0038	1.6782×10^{-8}	5.2928×10^{-6}	1.0116×10^{6}
210Hz	0.0037	1.6214×10^{-8}	4.8312×10^{-6}	9.8129×10^{5}
220Hz	0.0036	1.5464×10^{-8}	4.3974×10^{-6}	9.5099×10^{5}

Finally, the output voltage can then be calculated using equation (39) using the maximum stress value obtained. Table 4.4 summarizes the value of the output voltage obtained.

Table 4.4: Output voltage for every frequency

Actual Frequency	Beam length, l (µm)	Output voltage (V)
200Hz	4340	0.0223V
210Hz	4210	0.0216V
220Hz	4080	0.0209V

It is shown in Table 4.4 that as the beam length increases, the calculated output voltage of the cantilever power generator increases as well.

4.1.3   Cantilever Sensitivity

The cantilever design presented in this project is varied against its beam length. A MATLAB graph was done to see the effect of the output voltages against beam length. Figure 4.2 shows the graph between beam length (µm) for a range of against output voltage (V).
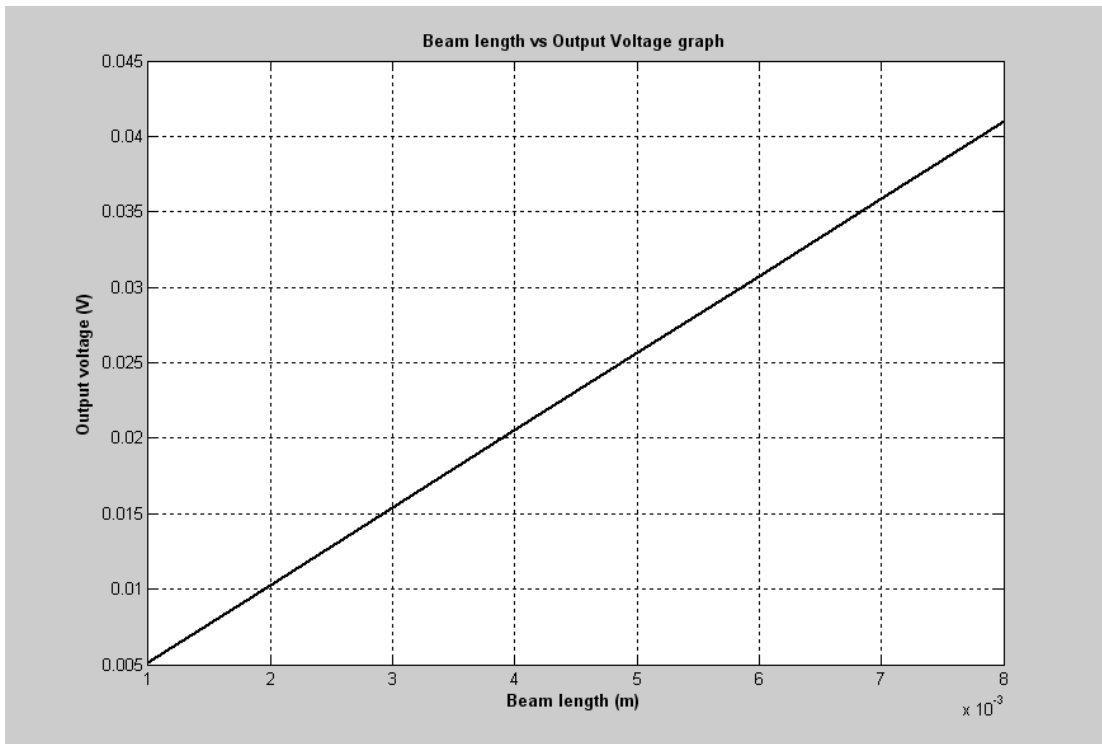
Figure 4.2: Beam length (µm) versus Output voltage (V) graph

It can be observed from Figure 4.2 that the output voltages calculated is directly proportional to beam length. The device sensitivity that is obtained from the slope of the graph is 5.13 V/mm.

4.2 CoventorWare Simulations

The finalized beam dimension for each range is used to create a beam design in the ConventorWare for beam characteristics simulation. The frequency range chosen are 200Hz, 210Hz and 220 Hz for each corresponding beam length of 4340µm, 4210µm and 4080µm. Other geometry parameters for the beam and the Nickel mass remains unchanged.

The steps involved in making the beam design in CoventorWare are as follows:

1) The material properties that are used in the design must be keyed into the Material Properties Database (MPD). This is important to define the characteristics of the materials that will be used in the design. The device characteristics that are being considered for this project can be viewed in Table 3.2. Figure 4.3 shows a sample look on the MPD editor.
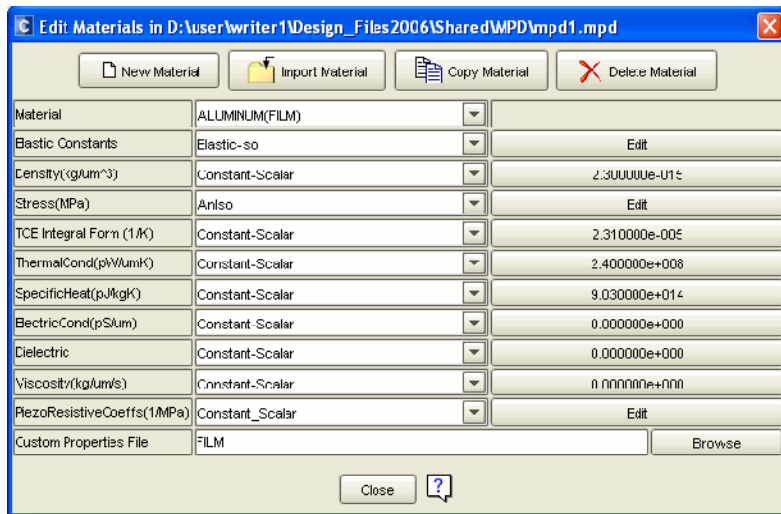
Figure 4.3: A sample look of the MPD

2) The layout of the beam design is created using the Layout Editor. This is to define the beam geometry and well as to define the mask used for the

fabrication pattern of each layer. Figure 4.4 shows the layout design done for the project.

Figure 4.4: Layout of the cantilever power generator design

3) The Process Editor defines the process that will be subjected to the design layers following the mask that has been used in the Layout Editor. The Process Editor will also identify the types of resist to be used, etching depth and the sidewall angle to the used. Figure 4.5 shows the process steps for the project design.

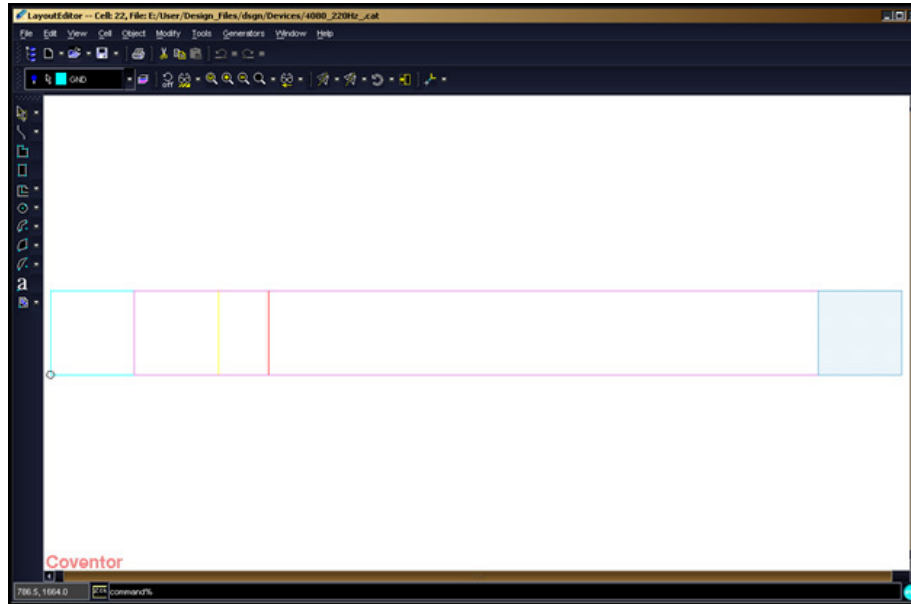| Number	Step Name	Action	Layer Name	Material Name	Thickness	Mask Name	Photoresist	Etch Depth	Mask Offset	Sidewall Angle
0	Substrate	Substrate	Substrate	SILICON	5	GND				
1	Planar Fill	Planar Fill	sacr	BPSG	600					
2	Generic Dry Etch	Straight Cut				Sacrifice	+		0	0
3	Generic Dry Etch	Straight Cut				Sacrifice1	+		0	70
4	Planar Fill	Planar Fill	poly	POLYSILICON	15					
5	Conformal Shell	Conformal Shell	SiO2	OXIDE	2					
6	Conformal Shell	Conformal Shell	bottom_Pt	PLATINUM	0.3					
7	Conformal Shell	Conformal Shell	piezo	PZT	2					
8	Generic Dry Etch	Straight Cut				Piezo	+		0	0
9	Conformal Shell	Conformal Shell	top_Pt	PLATINUM	0.3					
10	Generic Dry Etch	Straight Cut				Piezo	+		0	0
11	Conformal Shell	Conformal Shell	Ni_mass	NICKEL	200					
12	Generic Dry Etch	Straight Cut				Nic_mass	+		0	0
13	Delete	Delete		BPSG						

Figure 4.5: The process steps used for the cantilever power generator design

4) Using the process and layout files created for the design, the solid model of the beam design can now be created using the Preprocessor. The solid model design will adhere to the specification and conditions set by the layout and process files. Figure 4.6 shows the solid model of the beam design that have been built from the settings in Layout Editor and Process Editor.
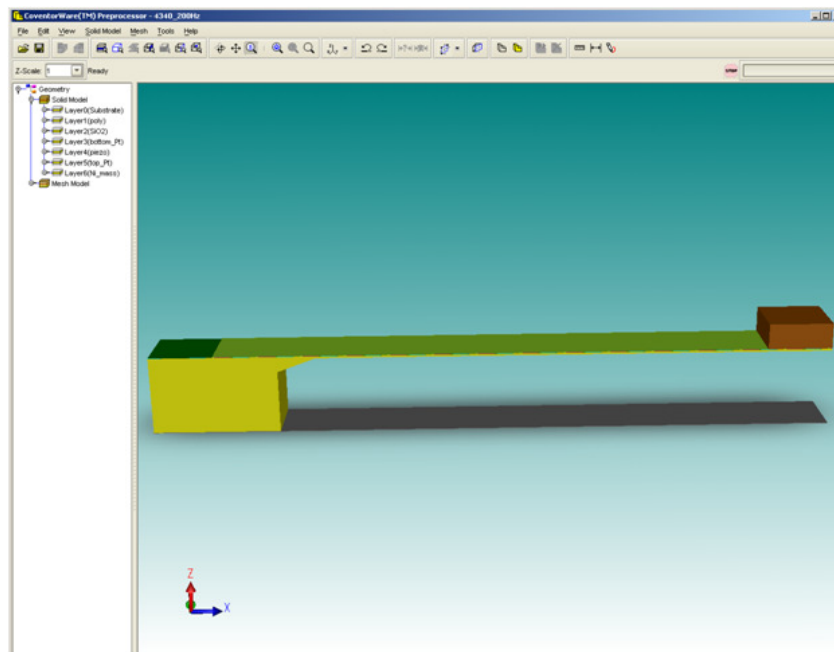

Figure 4.6: The solid 3D model of the cantilever power generator design.

38

It can be seen in Figure 4.5 that the main substrate of the device is Poly-silicon with is indicated in yellow. A close look on the other layers is shown in Figure 4.7.
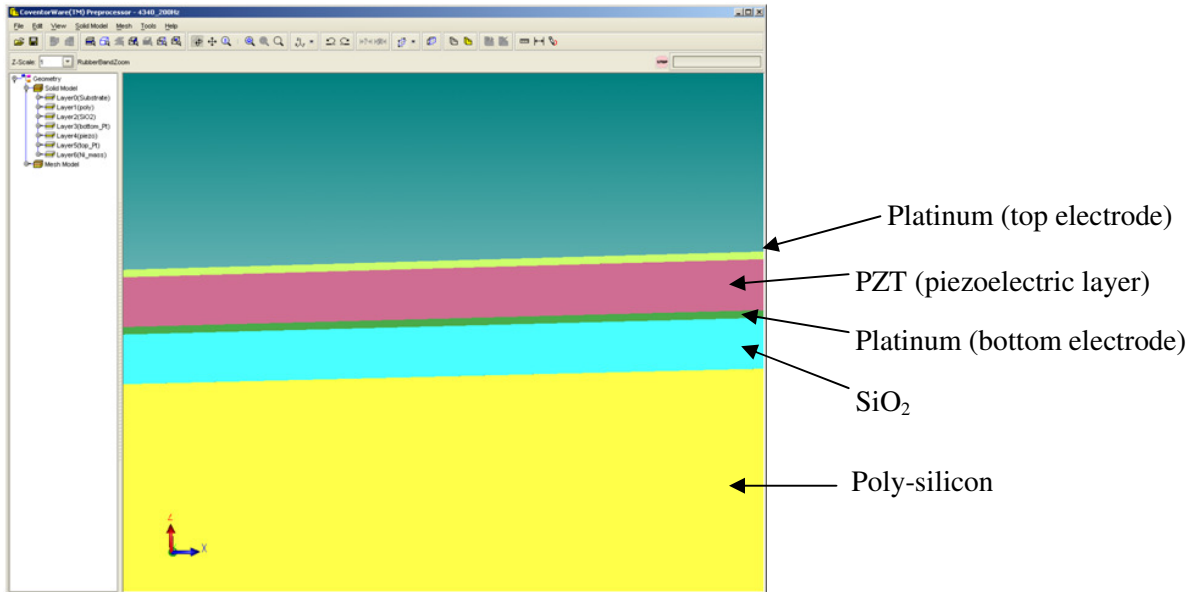
Figure 4.7: Component layers on the piezoelectric generator

5) In the Preprocessor, meshing was created to carry out the Finite Element Method (FEM) simulation. The type and the size of mesh was defined prior to meshing. The smaller the size of the element, the longer it takes for simulation process to be done. Figure 4.8 shows the meshing settings for the cantilever.
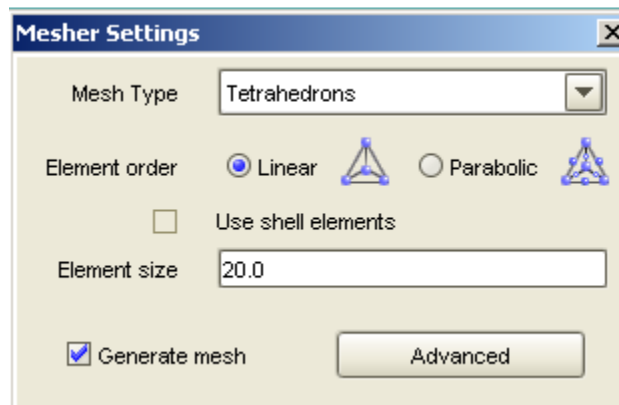

Figure 4.8: Mesher setting for the cantilever power generator

The meshed 3D model of the design is shown in Figure 4.9 where only the beam segment is meshed for FEM simulation. This is to reduce simulation time where only the moving part of the design is considered for FEM.

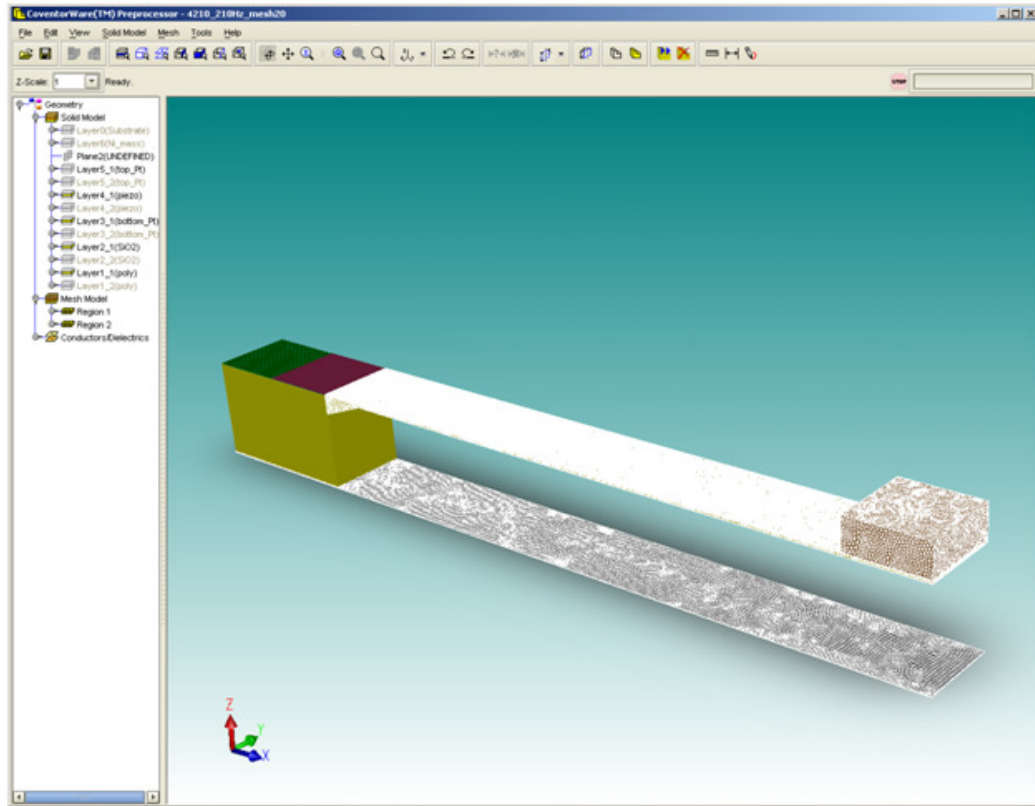**Figure 4.9**: Meshed 3-D layout of beam solid model

6) The meshing model design can then be subjected to one of the Analyzer solvers to simulate the characteristics of the beam cantilever. One of the solvers used are MemMech which mechanical characteristics of the design such as deflection, stress and frequency. Figure 4.10 shows the deflection of the design beam after being subjected to MemMech solver.
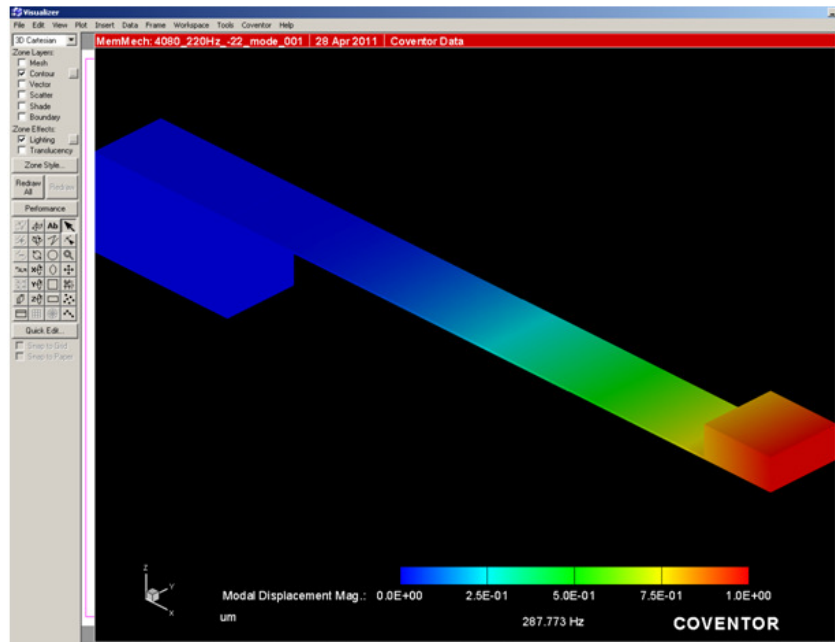
Figure 4.10: The beam deflection of the cantilever power generator

Based on the Figure 4.10, the beam deflection is indicated at the color scale of the model which is about 1µm. The stress experienced by the beam is shown in Figure 4.11. It can be observed that most of the stress exerted on the beam is located on at the point where the anchor and the length of the beam meets.
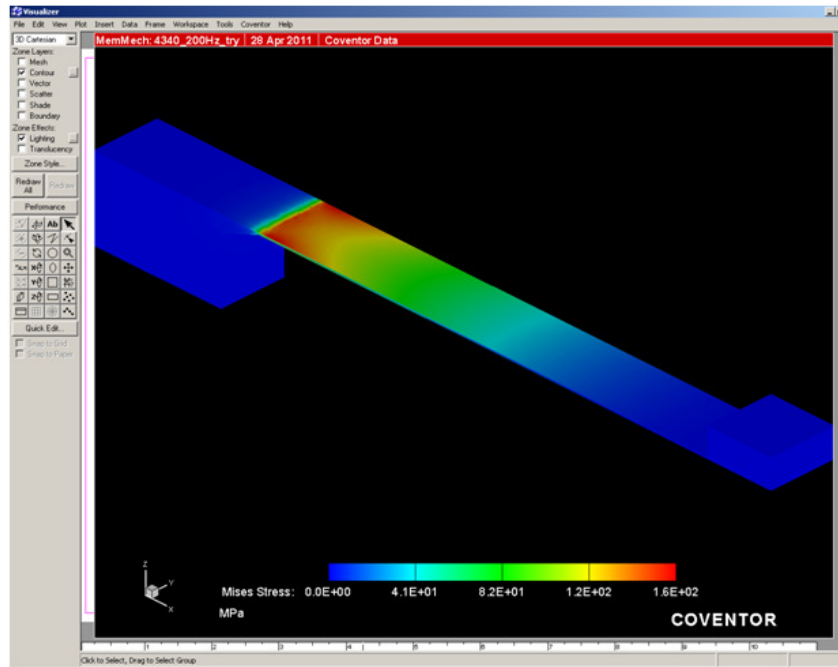
Figure 4.11: Stress location experienced by the beam

The stress location indicates the area where the piezoelectric effect experienced by the piezoelectric layer. The more stress exerted on the piezoelectric layer, the more charges it will produce thus creating more power.

The frequency of the beam was also simulated to obtain the desired frequency calculated in the mathematical analysis. Figure 4.12 shows the simulation frequency obtained for beam length 4340µm, 4210µm and 4080µm.

(a) Frequency for beam length 4340µm

(b) Frequency for beam length 4210µm

(c) Frequency for beam length 4080µm

Figure 4.12: Simulated frequency beam length for (a) 4340µm, (b) 4210µm and (c) 4080µm

Based on Figure 4.12, there is a percentage difference between the simulated frequency and the calculated frequency with respect to beam length. The difference could be caused by a difference in parameter and constants (such as Young's Modulus) or additional calculations made by the FEM that was not considered in the mathematical analysis. The percentage difference between the simulated and calculated frequency values is shown in Table 4.5.

Table 4.5: Percentage difference between the simulated and calculated frequency

Simulated frequency	Calculated frequency	Percentage difference
259 Hz	200 Hz	29.5%
263 Hz	210 Hz	25.2%
287 Hz	220 Hz	30.4%

CHAPTER 5

CONCLUSION AND RECOMMENDATION

5.1 Conclusion

A study on the design and simulation of the MEMS-based piezoelectric power generator has been conducted. Based on the mathematical modeling done, the array of the cantilever beam that can be used to create a wider frequency bandwidth for energy harvesting have been identified to be 4340µm, 4210µm and 4080µm in beam length to obtain 200Hz, 210Hz, and 220Hz frequency respectively. Simulation using the *CoventorWare* on the device characteristics shows that the simulated beam frequency needs a bit of improvement with a percentage difference of 25-30%. The calculated output voltage for each beam frequency is between the range of 0.0223-0.0209V.

The output circuit have been studied for this design, which is the three phase full wave rectifier, is selected especially to address the different phases that would produced by the piezoelectric power generator.

In conclusion, MEMS-based piezoelectric power generator is one of the possible solutions in giving power supply to wireless actuators and nodes. It presents an endless supply of electrical energy, provided that it is functioning well and its ability to make use of the vibration energy from the surrounding makes it an environmental friendly device.

5.2   Recommendations

The project was done in a specific time period thus not all design specifications was managed to be executed. Below are few recommendations that can be performed to continue on the project.

(a) Further simulations can be done to simulate the output voltages of the beam in CoventorWare.

(b) The calculated output voltage is not sufficient to power the output circuit. Thus, the steps below could be taken to solve the problem:

- Add more cantilever array arranged in series, to overcome the threshold voltage of the output circuit.
- Add a voltage multiplier to prior to the output circuit to amplify the voltage produced.

(c) Another round of optimization process can be executed to improve the output voltages so that the desired output voltage can be achieved.

REFERENCES

[1] Arnau A. V., 2008, *Piezoelectric Transducers and Applications* 2nd edition, Berlin, Springer

[2] Satoru Fujishima, (2000) "The History of Ceramic Filters", IEEE Transactions on Ultrasonics, Ferroelectrics and Frequency Control, Vol. 47, No. 1, January 2000.

[3] Ljubisa Ristic and Mahesh Shah, "Trends in MEMS Technology", IEEE Xplore Transactions, retrieved on July 29, 2010.

[4] Aliza Aini Md Ralib, Anis Nurashikin and Hanim Salleh, (2009) "Fabrication Techniques and Performance of Piezoelectric Energy Harvesters", ICEE International Conference on Energy and Environment 2009.

[5] Jing-Quan Liu, Hua-Bin Fang, Zheng-Yi Xu, Xin-Hui Mao, Xiu-Cheng Shen, Di Chen, Hang Liao and Bing-Chu Cai, (2008) "A MEMS-based piezoelectric power generator array for vibration energy harvesting", Microelectronics Journal 2008 (p.802-806).

[6] Eduard du Toit, N. 2005, *Modeling and Design of a MEMS Piezoelectric Vibration Energy Harvester*, Msc. Thesis, Massachusetts Institute of Technology, United States of America.

[7] Hua-Bin Fang, Jing-Quan Liu, Zheng-Yi Xu, Lu Dong, Li Wang, Di Chen, Bing-Chu Cai and Yue Liu, (2006) "Fabrication and performance of MEMS-based piezoelectric power generator for vibration energy harvesting", Microelectronics Journal 2006 (p.1280 – 1284).

[8] S. C. Lin, B. S Lee, W. J. Wu and C. K. Lee, (2009) "Multi-cantilever piezoelectric MEMS generator in energy harvesting", IEEE International Ultrasonics Symposium 2009.

[9] Y. B. Jeon, R. Sood, J.-h. Jeong and S. –G, Kim, (2005) "MEMS power generator with transverse mode thin film", Sensor and Actuators 2005 (p.16-22).

[10] B. Xu, Y. Ye, L. E. Cross, J. Berstein and R. Miller, (1999) "Dielectric hysteresis from transverse electric fields in lead zirconate titanate thin films", Appl. Phys. Lett. 74 (p. 3549-3551)

[11] J. J. Berstein, J. Bottari, K. Houston, G. Kirkos, R. Miller, B. Xu, Y. Ye and L. E. Cross, (1999) "Advanced MEMS ferroelectric ultrasound 2D arrays", IEEE Ultrasonics Symposium 1999.

[12] Shih-Nung Chen, Gou-Jen Wang and Ming-Chun Chien, (2006) "Analytical modeling of piezoelectric vibration-induced micro power generator", Mechatronics 2006 (p.376-387).

[13] Explain That Stuff. 19 Sept 2010;
http://www.explainthatstuff.com/piezoelectricity.html

[14] Inman D. J, 2008, *Engineering Vibrations* 3rd edition, New Jersey, Prentice Hall

[15] Balachandran B. and Magrab E. B, *Vibrations*, United States of America, Thomson & Brooks/Cole

[16] Nicolae O. Lobontiu, 2004, *Mechanical Design of Microresonators*, Digital Engineering Library @ McGraw-Hill (www.digitalengineeringlibrary.com)

[17] N. Lobontiu and E. Garcia, *Mechanics of Microelectromechanical Systems*, Kluwer Academic Press, New York, 2004.

[18] Wikipedia, 27th April 2011;
http://en.wikipedia.org/wiki/Euler%E2%80%93Bernoulli_beam_equation

[19] Irvine, Tom; 26th April 2011;
http://www.vibrationdata.com/tutorials2/beam.pdf

[20] 27th April 2011; http://courses.washington.edu/me354a/chap3.pdf

[21] Park, Jung-hyun, 2010, *Development of MEMS Piezoelectric Energy Harvester*, Ph.D Thesis, Auburn University, Alabama, United States of America.

[22] *Using CoventorWare manual*, 2007

[23] Hela Bousetta, Marcin Marzencki, Yasser Ammar and Skandar Basrour, (2007) "Multilevel Modeling of Integrated Power Harvesting System using VHDL-AMS and SPICE", IEEE Transaction 2007.

[24] MEMSnet. 31st November 2010; http://www.memsnet.org/material/

[25] Y. C. Shu and I. C. Lien, (2006) "Analysis of power output for piezoelectric energy harvesting systems", Smart Mater. Struct. 15 (p.1499-1512).

[26] PEC World. 15th March 2011
http://pecworld.zxq.net/Software/multisim/details/17_Single-Phase_full-Wave_Rectifiers.htm

[27] Industrial Electronics.com; *Three phase full wave rectifier*; 27th April 2011
http://www.industrial-electronics.com/Industrial_Power_Supplies_Inverters_and_Converter/6_Three-Phase-Full-Wave-Rectifier.html
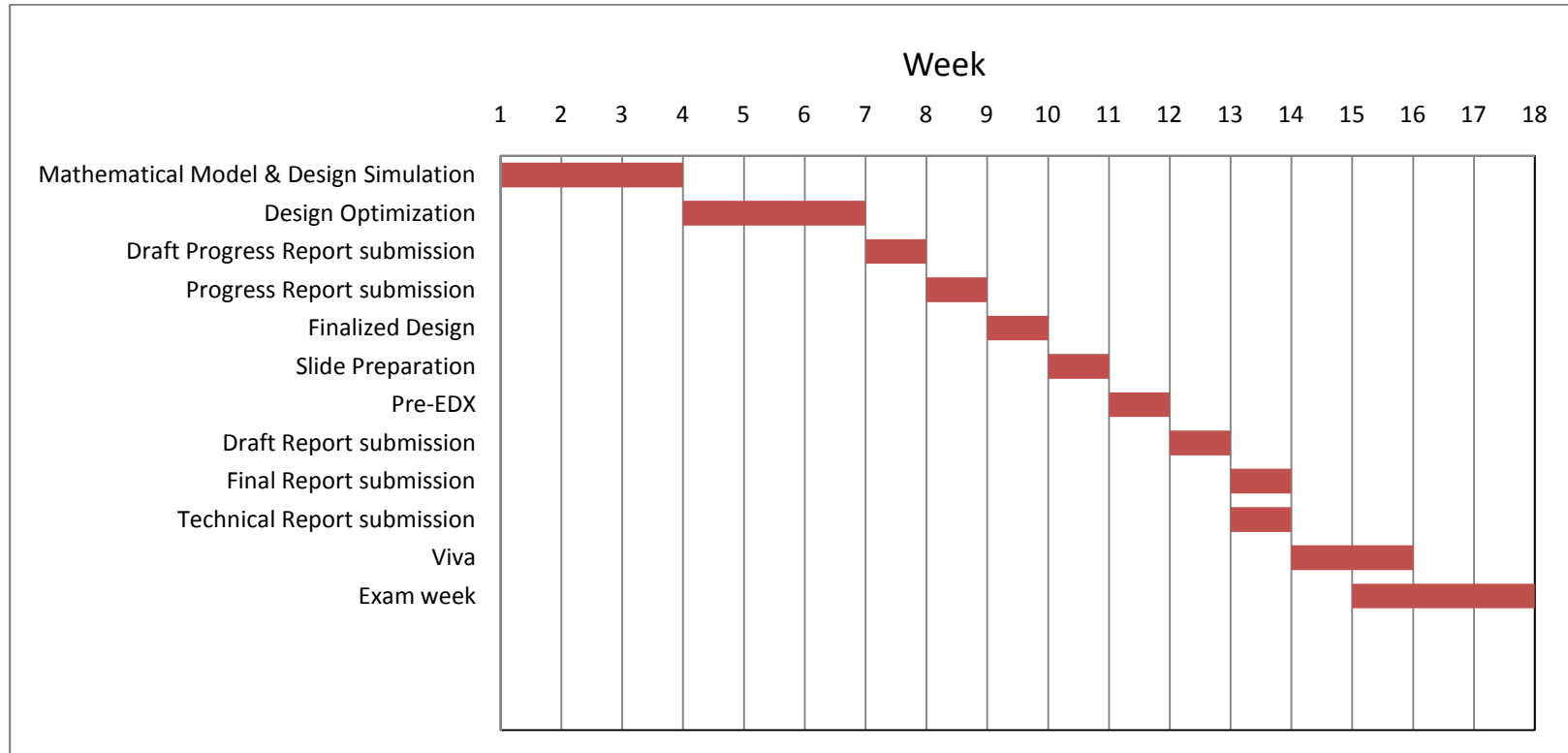
APPENDICES

APPENDIX A(1)

Gantt Chart for Final Year Project I
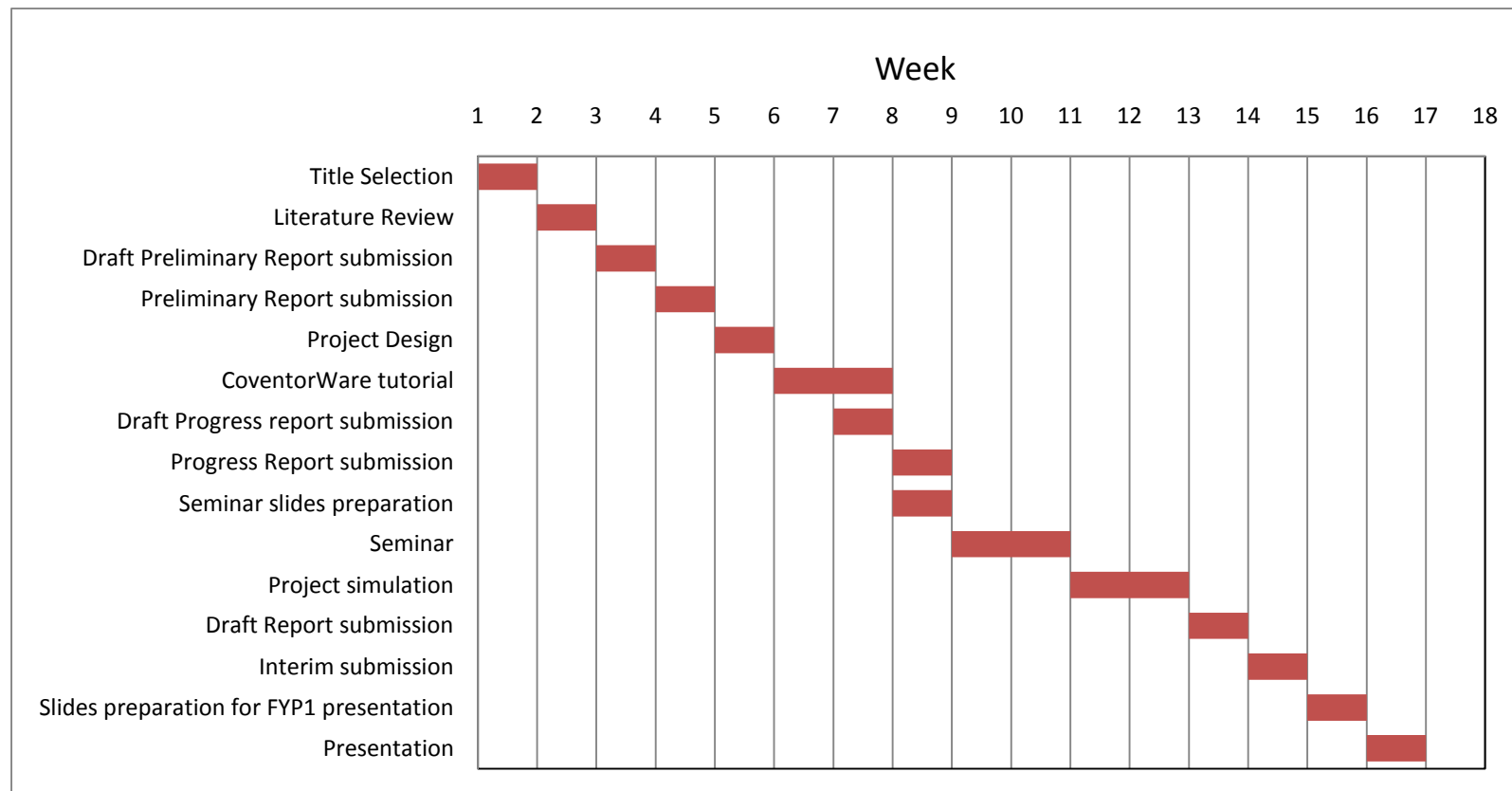
Gantt Chart for Final Year Project II

APPENDIX B

MATLAB script for bending frequency and output voltage for the power generating cantilever.

The following MATLAB script is used to calculate the bending frequency based on the beam dimensions for beam length of 4000µm.

```matlab
% Dimensions

L=4080e-6;
W=500e-6;

t_Pt=0.3e-6;
t_PZT=2e-6;
t_Ox=2e-6;
t_Ply=15e-6;

d_Pt=21400;   %top Pt electrode density
d_PZT=7600;   %PZT density
d_Ox=2200;    %SiO2 density
d_Ply=2330;   %Poly-si density
d_Ni=8910;    %Nickel density

e_Pt=145e9; %top Pt
e_PZT=89e9; %PZT
e_Ox=75e9;   %SiO2
e_Ply=160e9;%Poly-si

n_l=500e-6;
n_w=500e-6;
n_t=200e-6;


% Stiffness of beam


k=(e_Ply*W*t_Ply^3)/(4*L^3)



% Effective mass of beam

m=d_Ply*L*W*t_Ply
```

```matlab
n_m=d_Ni*n_l*n_w*n_t

comb_m=m+n_m;


% Frequency of beam wit added mass
f=(sqrt(k/comb_m))/(2*pi)


%Bending moment
g=9.81; %acceleration of gravity
b_mo=n_m*g*(L-n_l)

Lm=L-n_l


%Beam deflection
Y=(4*n_m*g*L^3)/(e_Ply*W*t_Ply^3)


%Max stress
m_st=(3*e_Ply*t_Ply*Y)/(2*L^2)


%Voltage output
g31=0.011; %piezoelectric voltage constant (Vm/N)

v_out=g31*m_st*t_PZT
```